LAWRENCE
LIVERMORE
NATIONAL
LABORATORY

LLNL-JRNL-404496

High resolution soft x-ray spectroscopy of low Z K-shell emission from laser-produced plasmas

J. Dunn, E. W. Magee, R. Shepherd, H. Chen, S. B. Hansen, S. J. Moon, G. V. Brown, M.-F. Gu, P. Beiersdorfer, M. A. Purvis

June 6, 2008

Review of Scientific Instruments

Disclaimer

High resolution soft x-ray spectroscopy of low Z K-shell emission from laser-produced plasmas

J. Dunn, [a] E.W. Magee, R. Shepherd, H. Chen, S.B. Hansen, S.J. Moon, G.V. Brown, M.-F. Gu, and P. Beiersdorfer

Lawrence Livermore National Laboratory, Livermore, CA 94551, USA

M.A. Purvis

NSF ERC for Extreme Ultraviolet Science and Technology, and Department of Electrical and Computer Engineering, Colorado State University, Fort Collins, Colorado 80523, USA

A large radius, R=44.3 m, High Resolution Grating Spectrometer (HRGS) with 2400 line/mm variable line spacing has been designed for laser–produced plasma experiments conducted at the Lawrence Livermore National Laboratory Jupiter Laser Facility. The instrument has been run with a low-noise, charge-coupled device detector to record high signal-to-noise spectra in the 10 – 50 Å wavelength range. The instrument can be run with a 10 – 20 μm wide slit to achieve the best spectral resolving power, approaching 1000 and similar to crystal spectrometers at 12 – 20 Å, or in slitless operation with a small symmetrical emission source. We describe preliminary spectra emitted from various H-like and He-like low Z ion plasmas heated by 100 – 500 ps (FWHM), 527 nm wavelength laser pulses. This instrument can be developed as a useful spectroscopy platform relevant to laboratory-based astrophysics as well as high energy density plasma studies.

Contributed paper published as part of the proceedings of the 17th Topical Conference on High Temperature Plasma Diagnostics, Albuquerque, New Mexico May 2008.

[a] Electronic mail: dunn6@llnl.gov

I. INTRODUCTION

The soft x-ray region has been an important spectral window for observing emission from various types of hot plasmas. Important plasma parameters from laboratory sources, for example laser-produced plasmas, magnetically-confined plasmas, and pinches, as well as solar corona and astrophysical sources can provide information on the plasma ion species, degree of ionization, temperature and density [1 – 6]. These parameters can be determined from the measurements and characterization of line and continuum emission. Furthermore, insight into the physical processes can be gained from the detailed study of the spectral features. In many cases for the study of plasmas emitting L-shell $n = 3 – 2$ lines of Fe and K-shell $n = 2 – 1$ lines of lower Z materials like oxygen or carbon are of interest, the x-ray spectral region falls in the 12 – 50 Å. Spectrometers based on Bragg diffraction analyzers are the preferred choice below ~20 Å and Acid Phthalate crystals can deliver spectral resolving power $\lambda/\Delta\lambda \sim 800$ [7]. Grating instruments have traditionally been used above 20 Å but have lower reflectivity and spectral resolution at lower wavelengths. Grating spectrometers, for example 1200 line/mm flat-field variable-spaced instruments [8] can have high resolving powers of several thousand when used with fine grain film in the 40 – 300Å range. Flat-field gratings with 2400 line/mm variable-spaced rulings can be used very effectively as survey diagnostics in the 10 – 70 Å region with lower resolving power of a few hundred with a charge-coupled device (CCD) detector [9].

A large radius of curvature $R = 44.3$ m 2400 line/mm variable-spaced grating spectrometer was recently constructed for measurements of soft x-rays emitted from the Lawrence Livermore National Laboratory Electron Beam Ion Trap (EBIT) in order to increase the instrument resolving power, typically 600 at 16 Å and 1200 at 35 Å [10]. In this work a second large radius instrument has been designed, built and optimized for laser-produced plasma studies

in order to measure spectral lines with high precision and study emission line wing shapes in the 12 – 50 Å range. Results from recent experiments will be discussed with a brief overview of future developments.

II. EXPERIMENTAL DESCRIPTION

A series of laser-produced plasma experiments were conducted at the Lawrence Livermore National Laboratory Jupiter Laser Facility to commission the high resolution grating spectrometer and make measurements of K-shell emission lines. The short pulse picosecond Compact Multipulse Terawatt (COMET) [11] and kilojoule Janus laser facilities were used. The COMET laser is a chirped pulse amplification table top system operating at 1054 nm fundamental wavelength that can provide a number of beams with pulse durations from 500 fs to 600 ps with a choice of 1ω or 2ω wavelengths. For this work, a 150 - 300 ps (FWHM), 527 nm wavelength pulses with up to 5 J energy on target was focused on target with an off axis parabola of focal length 30 cm. The laser could fire at a repetition rate of 1 shot/4 minutes. A maximum laser irradiance of 5×10^{15} W cm^{-2} was achieved with a sub 20 μm (FWHM) diameter vertically polarized laser beam incident on target at 21.8° from normal. The Janus laser campaign used higher laser energy 100 J in a 500 ps (FWHM) at 527 nm wavelength beam where the laser could fire once every 30 minutes. The laser was incident at 34° to target normal: The laser beam polarization was 30° from vertical and was focused with an *f*6 aspheric lens to various spot sizes from best focus to ~400 μm (FWHM) diameter. This gave a range of laser irradiances of 10^{13} - 5×10^{15} W cm^{-2}. Different targets including 1.5 μm and 3 μm thick Mylar ($C_{10}H_8O_4$) foils, 100 μm thick teflon (C_2F_4) and 50 mg cm^{-3} density aerogel (SiO_2) disks 1.4 mm diameter by 300 μm thick were irradiated to generate spectral emission lines of K-shell fluorine, oxygen and carbon. In both experiments the spectrometer viewed the target surface at a grazing angle of 5° in order

to minimize Doppler shift due to plasma expansion normal to the laser target. The Janus experimental layout is shown in Figure 1.

The spectrometer consisted of a variable-spaced grating of average ruling 2400 line/mm with radius of curvature R = 44.3 m. The spectrometer could be operated without a slit by placing the laser-produced plasma at the equivalent slit position. However, for these experiments, to minimize the effect of the source size on the instrument resolving power when the laser spot was defocused, a 25 μm wide slit was placed at a distance of 150 cm from the grating and 27.9 cm from the plasma for the Janus experiments. The slit was aligned horizontally and adjusted to be parallel to the grating using a fine adjustment rotation stage. A light tight 200 nm Al filter was placed behind the slit to prevent scattered light reaching the detector. The grating was inclined at a grazing angle of incidence of approximately 2° vertical to the source. The wavelength dispersion plane was in the vertical direction, out of the page in Fig. 1. A second plasma imaging slit 25 μm wide and oriented vertically was placed in front of the spectrometer slit and could be translated in front of the spectrometer. This gave spatially resolved spectra from the plasma plume expanding normal to the target surface with a magnification of 13.2× for the Janus experiments and 6.35× for the COMET experiments. A liquid-nitrogen cooled, back-thinned CCD with 1340 × 1300 pixels (pixel size 20 × 20 μm^2), operated at -110 °C, was used with a low noise analog-to digital-converter to record the spectra.

III. RESULTS

The COMET laser experiments were performed at best laser focus with a 150 ps, 527 nm wavelength, sub-20 μm focal spot with irradiances of approximately 5 × 10^{15} W cm^{-2}. Hydrodynamic simulations in 2-dimensions were performed using the code HYDRA [12] for the experimental laser conditions for a 3 μm thick Mylar ($C_{10}H_8O_4$) foil target. The simulations show

that the plasma electron temperature, T_e, reaches maximum values in excess of 1.6 keV on-axis, and at the peak of the laser pulse. These temperatures are sufficiently high to fully ionize the carbon and oxygen at the center of the focal spot. The plasma expands and rapidly cools down reaching temperatures of 300 eV at +200 ps and 80 – 100 eV at +400 ps relative to the peak of the laser pulse and after the laser pulse has ended. However, on the wings of the focal spot the temperature at the peak of the pulse is cooler $T_e \sim 300$ eV. This indicates that the emission lines are likely to come from different regions radially in the focal spot, in front of the target as the plasma expands and at different times.

The spectrometer was set up to study the K-shell oxygen, fluorine and carbon lines on different laser shots. The spectra reported here show oxygen resonance lines from the He-like $1s^2$ $^1S_0 - 1s2p\ ^1P_1$ at 21.6 Å through the He-like series limit to the H-like $1s\ ^2S_{1/2} - 3p\ ^2P_{1/2,\ 3/2}$ at 16.0 Å. The following spectra were spatially-integrated and were recorded from solid mylar foils and lower initial density aerogel targets as shown in Figure 2(a) and (b), respectively. The spectrometer viewing angle is chosen to minimize the Doppler shifts to the lines. The relation for the shifted wavelength follows as $\lambda = \lambda_o(1 + v_i\cos\theta/c)$ where λ_o is the rest frame wavelength, v_i is the emitting ion velocity, θ the viewing angle and c the speed of light [13] . The maximum estimated Doppler shift is -1.1 mÅ, blue-shifted, on the oxygen Ly-α line at 18.97 Å for an ion velocity of 2×10^7 cm s^{-1} and angle of 85° from normal. The spectra have high dynamic range with a signal-to-noise ratio of 5000 and spectral resolution of $\lambda/\delta\lambda > 1000$. This allows the observation of low intensity line features for example high n excited states and satellite lines to the O Ly-α transition that would not be clearly resolved by other instruments. Figures 3(a) and (b) show these low intensity line features in more detail. The steep drop in the continuum below 15.3 Å and above 22.6 Å is due to the edges of the detector. In Fig. 3(a) spectrum, the He-like

series limit is well-resolved for the Mylar target up to the $1s^2$ – 1s7p line. That transition appears broadened and is indicative of higher density than the aerogel target where the series limit is resolved to $1s^2$ – 1s8p, Fig. 3(b). While this is expected qualitatively, since the Mylar foil is starting from solid density and the maximum electron density for the aerogel target would be $n_e \sim 1.25 \times 10^{22}$ cm^{-3}, both targets have blown down substantially from the starting density due to the plasma hydrodynamic motion during and after the laser pulse. However an upper limit can be placed on the plasma density if one assumes that above a certain ion density continuum lowering results in a cutoff of excited *n* states [3]. A similar criterion can be used for Stark broadening [3]. An upper limit of 6×10^{20} cm^{-3} would be placed on the plasma density for both the Mylar and aerogel targets. The He-like $1s^2\ ^1S_0$ – $1s2p\ ^3P_1$ intercombination line at 21.8 Å is observed to the long side of the resonance line at 21.6Å. Since this line is collisionally quenched at increasing densities this confirms the above estimate that the He-like line emission is coming from the under dense plasma.

Other lines of interest include the dielectronic satellite lines to the O Ly-α in the waveband of 19.1 – 19.6 Å for the aerogel target in Fig. 3(b). These are resolved to better than one part in 1200. Precise measurement of the wavelengths with an accuracy better than ± 1 mÅ will allow testing of atomic structure models and comparison with previous data tables [14]. Figure 3(a) shows additional lines in the 19.5 – 21.5 Å band that are not observed in the aerogel spectrum. One possible explanation for these spectral features is that a higher Z contaminant may be present as a trace impurity [15] in the plastic. Identification of the lines is in progress. Further analysis is underway for spatially-resolved data where Stark-broadening of lines, dielectronic satellite line ratios and the ratio of the He-like intercombination line to the resonance lines can potentially be used as density and temperature diagnostics.

The second campaign on the Janus facility was designed to use the higher available laser energy to heat targets more uniformly with larger focal spots to reduce radial gradients in the focal spot. The target design was improved for the aerogel disks to have them nearly free-standing by mounting on a 500 nm thick polypropylene (C_3H_6) foil using a thin epoxy glue layer. The spectrometer spectral resolution was improved by optimizing the instrument geometry and slit size. The plasma emission was spatially imaged with 25 μm resolution in front of the target. Figure 4(a) shows a typical image of a spatially resolved oxygen spectrum emitted from an aerogel disk heated by a 500ps pulse focused to a large 400 μm spot at an irradiance of 10^{14} W cm^{-2}. The continuum emission is strongest close to the high density target surface and line emission is observed to extend out beyond 1 mm from the target surface. The five most intense resonance lines are labeled and all lines show substantial broadening near the target surface and a very narrow absorption feature at line center. This is strongly evident at the target surface but also extends out as far as 100 μm. Figure 4(b) shows spectral intensity lineouts at the target surface and at 100 μm. A combination of Stark and opacity broadening is washing out the He-like n = 3, 4 and 5 transitions at the target surface with the absorption feature helping to identify the line position. This indicates that the density is substantially higher than discussed earlier, for the spatially integrated aerogel spectra, but requires a complete treatment of the optical depth at line center. As the plasma density falls away from the target surface, for z=100 μm lineout in Fig. 4(b), the lines become optically thin: The absorption features and wing enhancement rapidly diminish. The interpretation of the spectral features is largely explained by opacity where photons in the line center are being absorbed and scattered out of the spectrometer field of view by cooler surrounding material in the line of sight. Similar results have been reported for carbon plasmas [16].

IV. CONCLUSIONS

A new, high resolution grating spectrometer has been built and used for laser-produced plasma studies. It has sufficient resolution and dynamic range to precisely measure spectral lines of various line intensities for comparison with atomic structure models. Line shape and wing studies. Future directions include the absolute calibration of the instrument spectral response and intrinsic line profile to be measured on EBIT. Further development of x-ray backlighters for absorption spectroscopy experiments and rapid heating of plasmas using short pulse heating beams are planned for the future.

ACKNOWLEDGMENTS

The authors would like to thank K. Cone, L. Elberson, J. Emig, J. Hunter, for experimental, technical and laser support as well as C. Cadwalader, R. Van Maren and J. Satcher for target fabrication. The help of the Jupiter Laser Facility staff is appreciated. The authors would like to thank M. Marinak for his helpful discussions regarding the code HYDRA. Part of this research was sponsored by the National Nuclear Security Administration under the Stewardship Science Academic Alliances program through U.S. Department of Energy Research Grant #DE-FG52-06NA26152. This work performed under the auspices of the U.S. Department of Energy by Lawrence Livermore National Laboratory under Contract DE-AC52-07NA27344.

REFERENCES

1. N.J. Peacock, M.G. Hobby, and M. Galanti, *J. Phys. B: Atom. Molec. Phys.* **6**, L298 – 304 (1973).
2. J. H. Parkinson, *Solar Physics* **42**(1), 183 (1975).
3. H.R. Griem, "Plasma Spectroscopy", (McGraw-Hill, New York, 1964).
4. C. De Michelis and M. Mattioli, *Nucl. Fus.* **21**(6), 677 (1981).
5. F.P. Keenan, S.M. McCann, R. Barnsley, J. Dunn, K.D. Evans, and N.J. Peacock, *Phys. Rev. A* **39**, 4092 (1989).
6. C.R. Canizares, D.P. Huenemoerder, D.S. Davis *et al.*, *ApJ.* **539**, L41 (2000).
7. A. Burek, *Space Sci. Instrum.* **2**, 53 (1976).
8. T. Kita, T. Harada, N. Nakano, and H. Kuroda, *Appl. Opt.* **22**, 512 (1983).
9. A. Saemann and K. Eidmann, *Rev. Sci. Instrum.* **69**, 1949 (1998).
10. P. Beiersdorfer, E.W. Magee, E. Träbert, H. Chen, J.K. Lepson, M.-F. Gu, and M. Schmidt, *Rev. Sci. Instrum.* **75**, 3723 (2004).
11. J. Dunn, Y. Li, A. L. Osterheld, J. Nilsen, J. R. Hunter, and V. N. Shlyaptsev, *Phys. Rev. Lett.* **84**, 4834 – 4837 (2000).
12. M.M. Marinak, S.W. Haan, T.R. Dittrich, R.E. Tipton, and G.B. Zimmerman, Physics of Plasmas, **5**(4), 1125 (1998).
13. J.C. Moreno, S. Goldsmith, and H.R. Griem, *J. Opt. Soc. Am. B* **9**(3), 339 (1992).
14. L.A. Vainshtein and U.I. Safronova, *At. Data and Nucl. Data Tables* 21, 49 (1978).
15. Similar spectral features in the 19.5 – 21.5 Å range were observed from a different laser-heated sample of 1.5 μm Mylar foil.

16. A.M. Malvezzi, L. Garifo, E. Jannitti, P. Nicolosi, and G. Tondello, *J. Phys. B: Atom. Molec. Phys.* **12**(2), 1437 (1979).

FIGURE CAPTIONS

Figure 1. Experimental schematic showing the high resolution grating spectrometer. An optional plasma imaging slit (vertical slit) is placed in front of the horizontal spectrometer slit. Wavelength dispersion is in the vertical direction. A CCD detector records the spectrum.

Figure 2. High resolution K-shell oxygen spectrum from laser-heated (a) 3 μm thick Mylar foil and (b) 300 μm thick 50 mg cm^{-3} aerogel target. Strongest line features in the He-like and H-like resonance lines are labeled.

Figure 3. Low intensity spectral features from Figure 2 are shown more clearly for (a) 3 μm thick Mylar foil and (b) 300 μm thick 50 mg cm^{-3} aerogel targets.

Figure 4. (a) Image of spatially-resolved oxygen K-shell spectrum of aerogel target irradiated with 500 ps laser pulse focused to approximately 400 μm spot diameter. Target surface is indicated at 0, plasma plume expands to the right and laser is incident from right. Dashed line signifies 100 μm in front of target surface. (b) Spectral intensity line outs at the target surface (z=0 μm), offset for clarity, and in front of the target (z=100 μm).

Fig. 1 Dunn *et al*

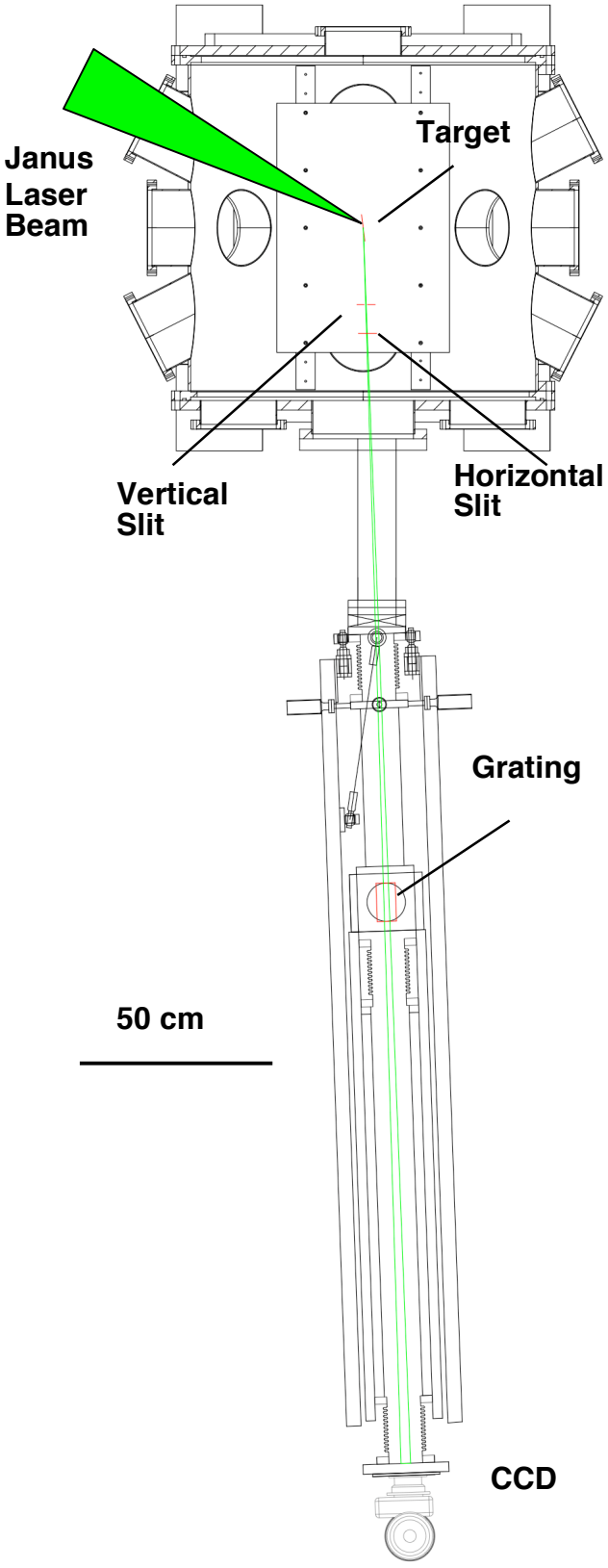

Fig. 2 Dunn *et al*

(a)

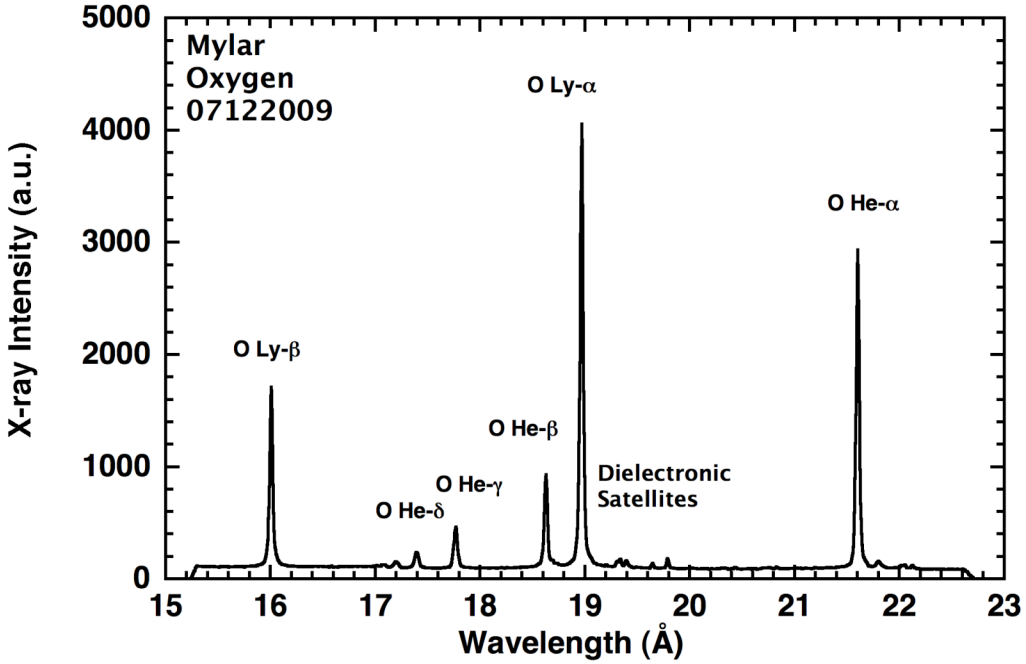

(b)

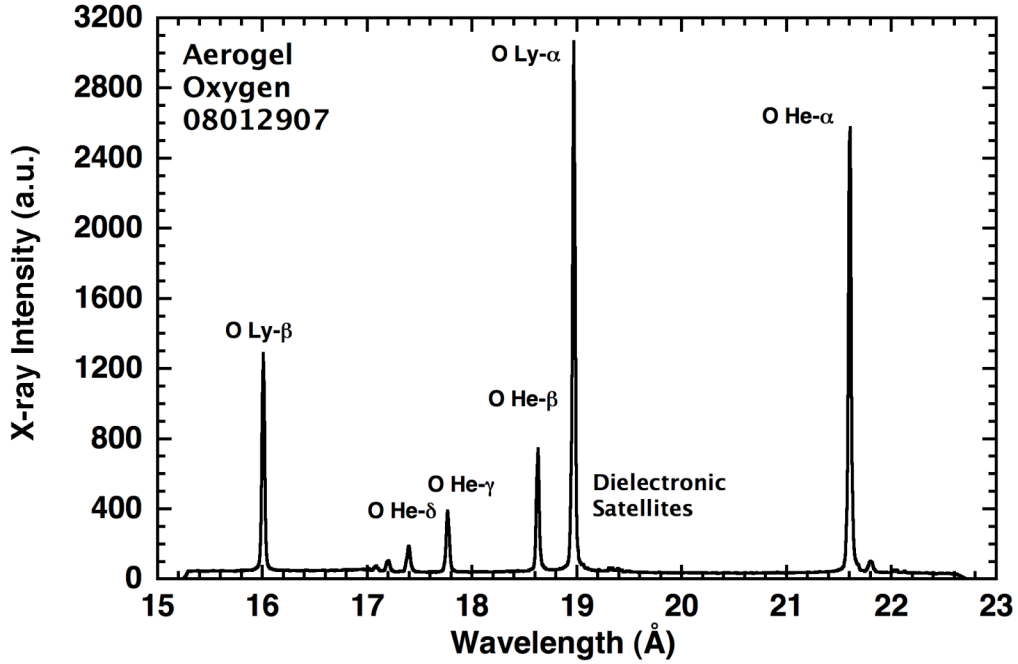

Fig. 3 Dunn *et al*

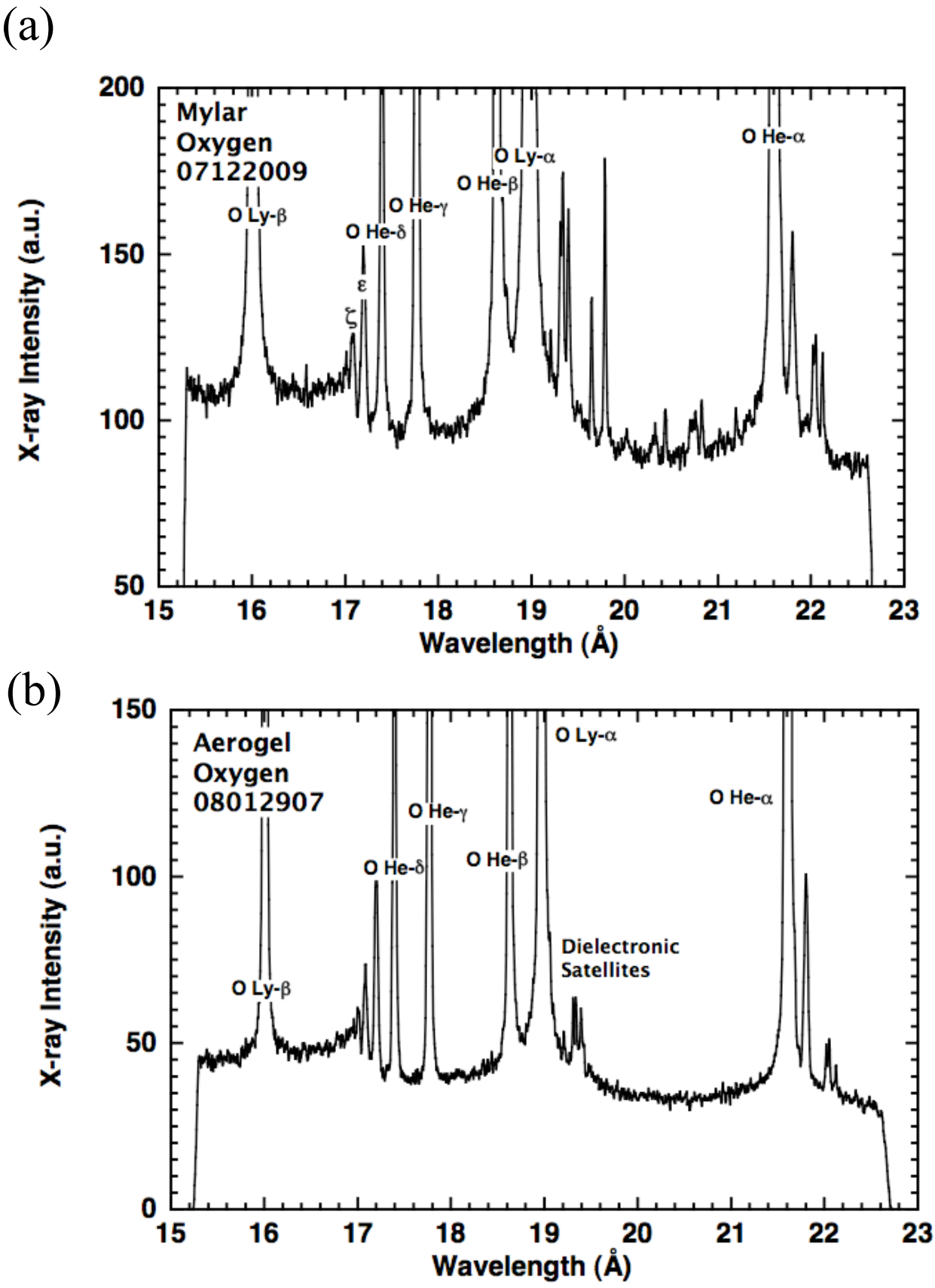

Fig. 4 Dunn *et al*